BRIEF REPORT

Mesenchymal Hamartoma of the Liver and DICER1 Syndrome

Maria Apellaniz-Ruiz, Ph.D., Maria Segni, M.D., Matthias Kettwig, M.D., Sylvia Glüer, M.D., Ph.D., Dylan Pelletier, Van-Hung Nguyen, M.D., Rabea Wagener, Ph.D., Cristina López, Ph.D., Karl Muchantef, M.D., Dorothée Bouron-Dal Soglio, M.D., Ph.D., Nelly Sabbaghian, M.Sc., Mona K. Wu, Ph.D., Stefano Zannella, M.D., Marc R. Fabian, Ph.D., Reiner Siebert, M.D., Jan Menke, M.D., Ph.D., John R. Priest, M.D., and William D. Foulkes, M.B., B.S., Ph.D.

SUMMARY

Mesenchymal hamartoma of the liver (MHL) is a benign tumor affecting children that is characterized by a primitive myxoid stroma with cystically dilated bile ducts. Alterations involving chromosome 19q13 are a recurrent underlying cause of MHL; these alterations activate the chromosome 19 microRNA cluster (C19MC). Other cases remain unexplained. We describe two children with MHLs that harbored germline *DICER1* pathogenic variants. Analysis of tumor tissue from one of the children revealed two *DICER1* "hits." Mutations in *DICER1* dysregulate microRNAs, mimicking the effect of the activation of C19MC. Our data suggest that MHL is a new phenotype of DICER1 syndrome. (Funded by the Canadian Institutes of Health Research and others.)

From the Departments of Human Genetics (M.A.-R., M.K.W., W.D.F.), Pharmacology (D.P.), Oncology (M.R.F., W.D.F.), and Biochemistry (M.R.F.), and the Lady Davis Institute, Segal Cancer Centre, Jewish General Hospital (M.A.-R., D.P., N.S., M.K.W., M.R.F., W.D.F.), McGill University, the Department of Pathology, Montreal Children's Hospital (V.-H.N.), the Department of Radiology (K.M.), and the Cancer Research Program, Research Institute (W.D.F.), McGill University Health Centre, and the Department of Pathology, Centre Hospitalier Universitaire Sainte-Justine (D.B.-D.S.) — all in Montreal; the Department of Pediatrics, Endocrinology Unit, Sapienza University, Rome (M.S.), and Centro Diagnostico Italiano, Milan (S.Z.) — both in Italy; the Department of Pediatrics and Adolescent Medicine, Faculty of Medicine (M.K.), and the Institute for Diagnostic and Interventional Radiology, Faculty of Medicine (J.M.), Georg-August University, Göttingen, the Department of Pediatric Surgery, St. Bernward Krankenhaus Hildesheim, Hildesheim (S.G.), and the Institute of Human Genetics, Ulm University and Ulm University Medical Center, Ulm (R.W., C.L., R.S.) — all in Germany; and Minneapolis (J.R.P.). Address reprint requests to Dr. Foulkes at the Cancer Genetics Laboratory, Lady Davis Institute, Segal Cancer Centre, Jewish General Hospital, 3755 Côte-Sainte-Catherine Rd., Montreal, QC H3T 1E2, Canada, or at william.foulkes@mcgill.ca.

Drs. Segni and Kettwig contributed equally to this article.

N Engl J Med 2019;380:1834-42.
DOI: 10.1056/NEJMoa1812169

Mesenchymal hamartoma of the liver (MHL), with a reported incidence of 0.7 cases per million population per year,[1] accounts for approximately 10% of liver tumors in persons younger than 21 years of age and is the second most common benign liver tumor in children, after hemangioma.[2] Children with MHL may present with an enlarging, painless abdominal mass; MHL typically manifests as a multicystic liver mass composed of disorganized arrangements of primitive mesenchyme, cysts lined with biliary-type epithelium, and hepatic parenchyma.[2] MHL is usually unaccompanied by other disorders, but associations with Beckwith–Wiedemann syndrome[3,4] and placental mesenchymal dysplasia[4] are documented. After surgical resection, the prognosis for MHL is excellent[4]; however, incomplete excision may be associated with malignant transformation to undifferentiated embryonal sarcoma.[4] Spontaneous regression has also been reported.[4]

Aberrant activation of the chromosome 19 microRNA cluster (C19MC), leading to dysregulated microRNA profiles, is often implicated in MHL.[5,6] Located on chromosome 19q13.4, C19MC encodes a paternally imprinted cluster of 46 primate-specific microRNAs expressed in placenta and also in certain cancers.[7] This microRNA alteration in MHL results from either androgenetic–biparental mosaicism (in which a subset of the person's cells has complete paternal uniparental disomy and the rest of the cells have one set of chromosomes derived from the mother and one from the father) or chromosomal rearrangements in the 19q13.4 region.[5,6,8] However, C19MC activation is not a universal property of MHLs, since a minority of cases lack C19MC expression.[6]

Dysregulated microRNAs also cause DICER1 syndrome (Online Mendelian Inheritance in Man #601200), a tumor predisposition syndrome that features several dysontogenetic cystic conditions in young children, most notably pleuropulmonary blastoma and cystic nephroma.[9] Multinodular goiter is the most frequent clinical manifestation.[9,10] Tumors occurring in this syndrome are characterized by biallelic pathogenic variants in *DICER1*: a germline variant (which typically results in loss of DICER1 function) accompanied by a characteristic somatic missense mutation that modifies one of five "hot spot" amino acids in the RNase IIIb domain (E1705, D1709, G1809, D1810, and E1813). In a person with DICER1 syndrome and multiple tumors, the somatic mutation in each tumor is likely to differ from that in other tumors.[11,12] Even within the multiple nodules of one person's multinodular goiter, the hot spots may differ between nodules, which indicates an independent molecular evolution of each nodule.[10,13] We studied two cases of MHL to explore the possibility that MHL is a phenotype of DICER1 syndrome. (Written informed consent to the analyses reported here was provided by the mother of Child 1 and both parents of Child 2. Both children signed minor assent forms.)

CASE REPORTS

CHILD 1

A 26-month-old boy presented with a cyst in the left hepatic lobe that measured 19 cm in the largest dimension (Fig. 1A; and Fig. S1A in the Supplementary Appendix, available with the full text of this article at NEJM.org). There was no evidence of biliary atresia; testing for parasites was negative, and liver-function tests were unremarkable. The mass was resected, but 4 months later, because of multiple recurrent and enlarging cysts, a hepatic lobectomy was performed, which revealed multiple cysts ranging from 1 to 4 cm in diameter. Pathological examination of both resection specimens identified partly fibrous and focally myxoid mesenchymal stroma with epithelial-lined cysts and nonepithelialized cystic spaces, as well as bile ducts, vessels, entrapped hepatocytes, and areas with extramedullary hematopoiesis, findings that led to a diagnosis of MHL (Fig. 1A, and Figs. S2 and S3 in the Supplementary Appendix). No further cysts have occurred in 13 years of follow-up. At 4 years 9 months of age, a 2-cm nodule in the right lobe of the thyroid was resected and diagnosed pathologically as follicular adenoma. During the next 9 years, five nodules in the left thyroid lobe were diagnosed as benign nodules after fine-needle aspiration. (For details, see the section on clinical data and Fig. S1B through S1D in the Supplementary Appendix.) The family history was unremarkable.

CHILD 2

In a male infant who was being followed closely for thoracic and abdominal disease (see below), magnetic resonance imaging at 9 months of age revealed a 14-mm solid liver tumor with enclosed tiny cysts (Fig. 1B). Subsequently, this lesion became polycystic without radiographically detectable solid residual, and its diameter had increased to 6.6 cm when the child was 39 months of age. Liver-function studies were normal. At 75 months of age, the child underwent a sonography-guided needle biopsy to rule out cancer. Pathological examination revealed portions of fibrous cystic wall lined by a single layer of cuboidal and attenuated epithelial cells with adjacent normal hepatic parenchyma, findings consistent with MHL. Subsequently, the hepatic cyst regressed substantially, and calcification was noted at 14 years of age (Fig. S4A through S4D in the Supplementary Appendix).

In addition to the hepatic disease, this child had other phenotypes of DICER1 syndrome: extensive bilateral pulmonary cysts diagnosed retrospectively as pleuropulmonary blastoma type I, jejunal hamartomatous polyps associated with intussusception, a right kidney cystic nephroma, a left renal cyst, and bilateral nodular thyroid disease. (For details, see the section on clinical data and Fig. S5 in the Supplementary Appendix.) In the right kidney, a polycystic structure recurred after removal of the cystic nephroma. These recurrent cysts and the left renal cyst regressed over time without intervention (Fig. S4E through S4I in the Supplementary Appendix). The thyroid disease was diagnosed as noninvasive follicular thyroid neoplasm with papillary-like nuclear features. The child's mother had pulmonary cysts removed twice in infancy and two thyroid surgeries as a teenager (Fig. 1B). His father's medical history was unremarkable.

METHODS AND RESULTS

MOLECULAR GENETIC ANALYSIS OF *DICER1*

Analysis of Child 1's germline DNA with the use of polymerase-chain-reaction (PCR) amplification and Sanger sequencing identified a heterozygous pathogenic germline *DICER1* variant (c.4007delC, p.P1336Lfs*11) (Fig. 2A, and the Methods section in the Supplementary Appendix). Analysis of thyroid tumor and MHL RNA

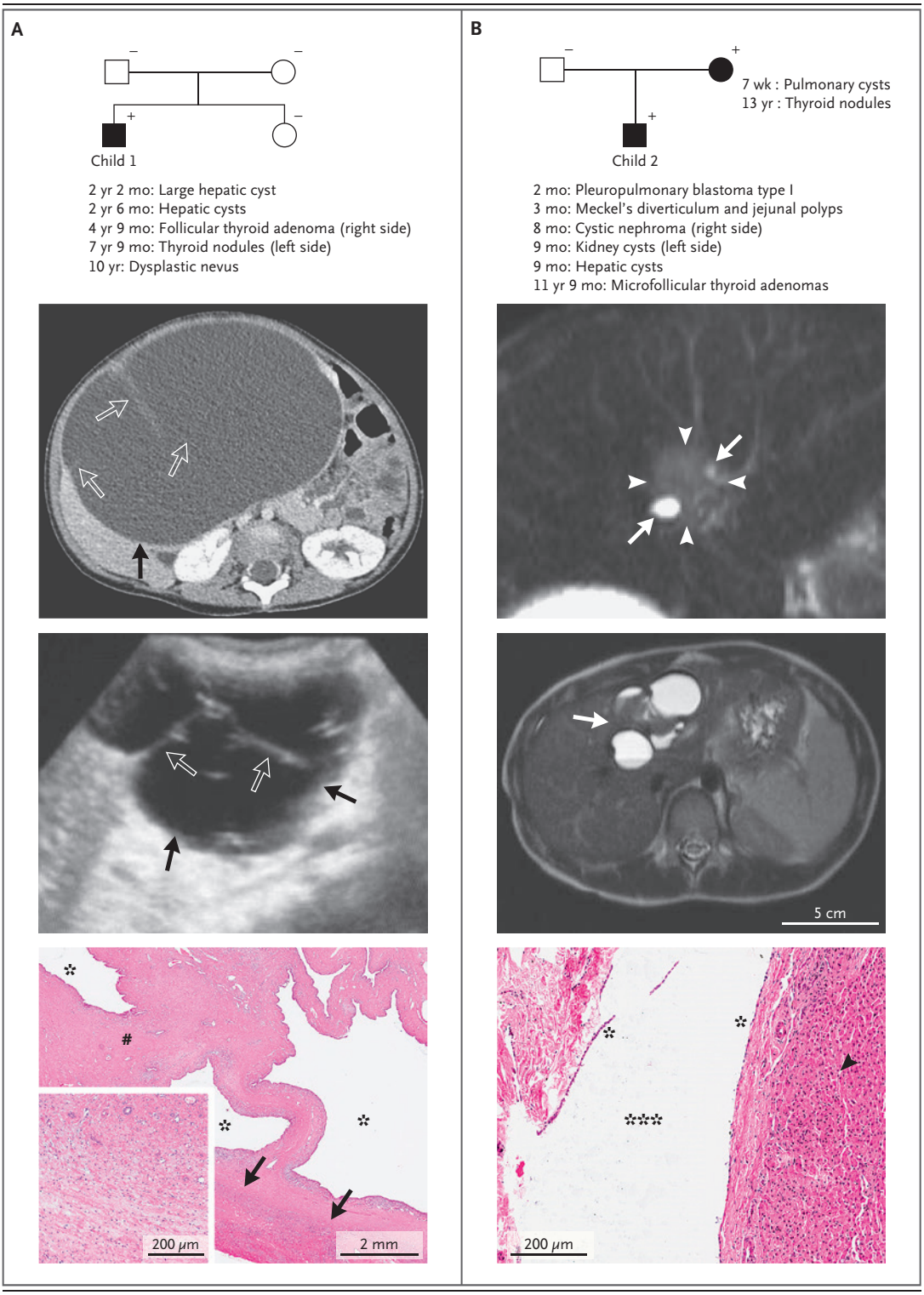

suggested that the mutant messenger RNA (mRNA) was targeted by nonsense-mediated decay, which would result in no mutant DICER1 protein being produced (Fig. S6A in the Supplementary Appendix). The child's parents and sister did not carry the variant, indicating its de novo origin. The thyroid nodule and MHL harbored somatic hot-spot RNase IIIb *DICER1* mutations (c.5125G→A, p.D1709N; and c.5113G→C, p.E1705Q, respectively) (Fig. 2A). Expression of c.5113G→C in the MHL was confirmed by droplet digital PCR assay (Fig. S6C in the Supplementary Appendix).

Screening of *DICER1* in germline DNA from Child 2 and his parents revealed that the child and mother were heterozygous for an in-frame germline deletion in *DICER1* (c.5225_5227delACA, p.N1742del) (Fig. 2B). The mutation is predicted to result in the deletion of a highly conserved amino acid in the RNase IIIb domain of the DICER1 protein (Fig. S7 in the Supplementary Appendix). As expected, the mutant mRNA was not subjected to nonsense-mediated decay (Fig. S6B in the Supplementary Appendix). Multiplex ligation-dependent probe amplification did not identify exonic rearrangements (data not shown).

Subsequently, we analyzed the DNA extracted from the pleuropulmonary blastoma, cystic nephroma, polyps, multinodular goiter, and liver cystic lesion. Tumor tissue from the child's mother was not available. The cystic nephroma and the pleuropulmonary blastoma carried typical somatic hot-spot mutations (c.5125G→A, p.D1709N; and c.5113G→A, p.E1705K, respectively) (Fig. 2B). The polyps and the multinodular goiter were also analyzed on a Fluidigm Access Array targeting *DICER1* exons, exon–intron boundaries, and 3′ untranslated region. In the multinodular goiter, we identified loss of heterozygosity of the wild-type allele within the tumor (Fig. 2B). Somatic mutations were not detected in either the polyps or the liver tissue. However, the material that was obtained from the hepatic biopsy was minimal, and most of the cells were normal hepatocytes.

Figure 1 (facing page). Pedigrees and Images of Multicystic Liver Lesions in Two Children.

Panel A pertains to Child 1 and Panel B to Child 2, with family pedigrees shown at the top. Squares indicate male family members, and circles indicate female family members; a plus sign indicates a person who is heterozygous for a *DICER1* pathogenic germline variant, and a minus sign indicates a person with wild-type *DICER1*. In Panel A, a transverse contrast-enhanced computed tomographic image at 2 years 2 months of age shows a 19-cm intrahepatic cystic mass (solid arrow) with septations (open arrows). An ultrasonographic image at 4 months after resection of the mass shows a recurrent multilocular cystic mass (solid arrows) with septations (open arrows). A representative hematoxylin and eosin–stained section of the mesenchymal hamartoma of the liver (MHL) shows a mainly multicystic lesion with epithelium-lined cysts (asterisks), vascularized collagenous fibrous stroma with entrapped bile ducts (pound sign), and compressed peripheral normal hepatic parenchyma (arrows). The inset shows an area of myxoid stroma and entrapped bile ducts from a different region of the MHL. (Additional histopathological images from Child 1 are provided in Figs. S2 and S3 in the Supplementary Appendix.) In Panel B, a transverse T_2-weighted magnetic resonance image (MRI) at 9 months of age (upper MRI) shows a 14-mm solid tumor (arrowheads) in liver segment 4 that contained tiny cysts (arrows). Numerous subsequent imaging studies (not shown) revealed an enlarging and ultimately regressing cystic mass with no apparent soft tissue component. (Measurements of cystic-mass size over time are provided in Fig. S4 in the Supplementary Appendix.) A transverse T_2-weighted MRI at 5 years of age (lower MRI) shows a multilocular intrahepatic cystic mass (arrow). A hematoxylin and eosin–stained section from the liver biopsy performed at 6 years of age shows a section of the epithelial lining of the cyst (one asterisk), the cystic space (three asterisks), and normal hepatocytes (arrowhead).

EFFECTS ON DICER1 FUNCTION AND MICRORNA EXPRESSION

To determine the effect of specific *DICER1* mutations on its catalytic activity, we took advantage of an in vitro DICER1 cleavage assay.[11] Briefly, immunoprecipitated DICER1 mutants were incubated with a ^{32}P-labeled precursor microRNA 122 (pre-miR-122) hairpin, and RNA cleavage products were visualized by means of autoradiography. As compared with wild-type DICER1 protein, which generates both 5p and 3p microRNAs, the p.E1705Q mutant (found in Child 1's MHL) did not correctly cleave the pre-miR-122 (Fig. 2C). Instead, it generated reduced levels of both 5p and 3p microRNAs, as well as an abnormal uncleaved 5p arm. Products from the 3p arm were reduced to a lesser degree. The hot-spot mutation p.D1709Y acted as a positive control for aberrant in vitro cleavage. The DICER1 p.N1742del mutant (identified in Child 2) also engendered abnormal pre-miR-122 processing (Fig. 2D).

We used a quantitative PCR assay to analyze the expression of four microRNAs expressed in the liver — miR-122-5p, miR-200a-3p, miR-199b-5p, and let-7a-5p (Fig. 2E)[14,15] — in the MHL from Child 1, three liver control samples, and one

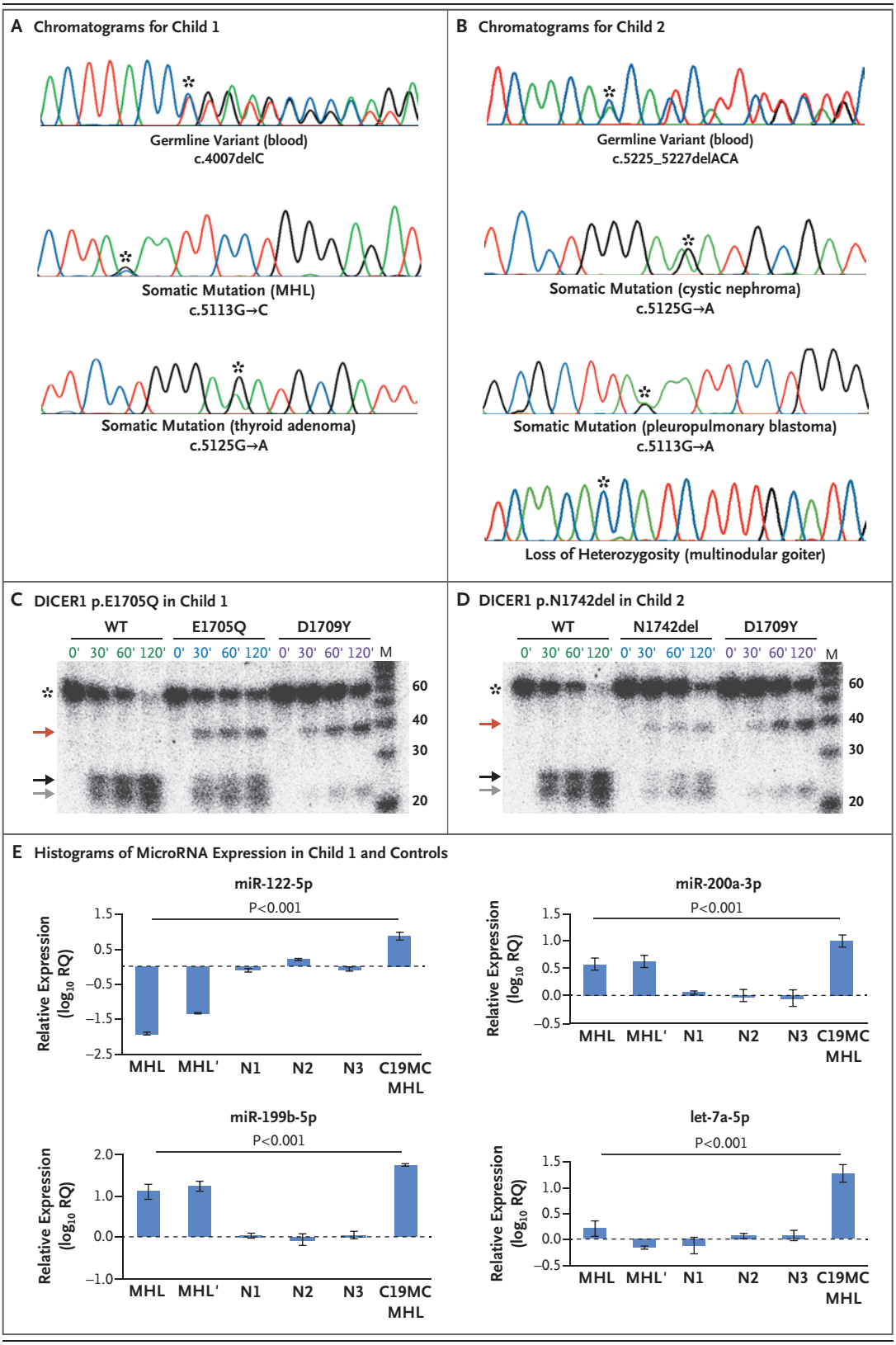

Figure 2 (facing page). *DICER1* Testing, In Vitro Cleavage Assays, and MicroRNA Expression.

Shown are sample chromatograms of *DICER1* genotypes in germline and tumor DNA obtained from Child 1 (Panel A) and Child 2 (Panel B). Sites of mutation or loss of heterozygosity are indicated by asterisks. Panels C and D show the results of in vitro cleavage assays for DICER1 proteins with the use of the precursor microRNA 122 (pre-miR-122) hairpin: DICER1 p.E1705Q in Child 1 and DICER1 p.N1742del in Child 2. DICER1 p.D1709Y was used as the hot-spot mutation–positive control. The pre-miR-122 hairpin was chosen because miR-122 is critically implicated in liver development. The expected pattern of cleavage is shown in wild-type (WT) DICER1, with increasing cleavage of the pre-miR-122 hairpin (marked with an asterisk) occurring over a period of 120 minutes, leading to a diminution of the intensity of the pre-miR-122 band at 60 nucleotides and increasing intensity of both 3p (bottom band, shown as gray arrow) and 5p (top band, black arrow) over the same period. Both DICER1 p.E1705Q and DICER1 p.N1742del showed aberrant patterns with production of an uncleaved 5p arm (red arrow, band at 40 nucleotides) and less 5p and 3p products, with the decrease of 5p being more pronounced. A radiolabeled RNA molecular-weight marker (M) was loaded in every assay. Panel E shows histograms of the relative levels of expression of four microRNAs measured by quantitative polymerase-chain-reaction (PCR) assay in two MHL samples from Child 1 (MHL from the first surgery and MHL′ from the second surgery), normal liver samples (N1, N2, and N3) from three separate persons, and an MHL with activation of the chromosome 19 microRNA cluster (C19MC) and no *DICER1* mutations (C19MC MHL). MHL samples from Child 1 showed altered microRNA expression as compared with C19MC MHL. The standard deviations of the cycle thresholds are plotted as I bars. Bonferroni-corrected P values for the comparison between MHL samples (MHL and MHL′) and C19MC MHL are shown; all P values are provided in Table S1 in the Supplementary Appendix. RQ denotes relative quantity.

non-*DICER1* mutated MHL sample. Statistical analysis of the data was performed with the use of one-way analysis of variance and followed by the Tukey test to adjust for multiple comparisons to identify the significant pairwise comparisons. We found that miR-122-5p was significantly down-regulated in Child 1's MHL as compared with three control samples of liver tissue and with a non-DICER1 C19MC-positive MHL (P<0.001 for all comparisons). We also found that miR-199b-5p and miR-200a-3p were overexpressed in Child 1's MHL as compared with the control liver samples (P<0.001), but the levels were lower than in the non-DICER1 MHL (P<0.001). Let-7a-5p was expressed in Child 1's MHL at the same level as in normal tissue; however, it was overexpressed in the non-DICER1 MHL (P<0.001).

C19MC MICRORNA EXPRESSION

Four MHL cases caused by androgenetic–biparental mosaicism have been reported, and chromosomal rearrangements involving 19q13 have been identified in 20 of 24 cytogenetically studied cases.[5,6,8] In Child 1, DNA from the MHL that was hybridized to an OncoScan single-nucleotide polymorphism array showed neither allelic imbalances nor uniparental disomy at any chromosomal loci, including 19q13.4; these results ruled out androgenetic–biparental mosaicism (Fig. 3A, and Fig. S8 in the Supplementary Appendix). Fluorescence in situ hybridization on the MHL tissue did not reveal rearrangements involving 19q13.4 (Fig. 3B). The expression of four C19MC microRNAs[7] (miR-512-1-3p, miR-520c-3p, miR-520g-3p, and miR-519a-1-3p) and miR-372-3p from a nearby region was measured by means of quantitative PCR assay in the MHL from Child 1, liver controls, and one MHL sample expressing C19MC microRNAs. Lower microRNA expression was seen in Child 1's DICER1-related MHL and normal liver samples than in the positive control (Fig. 3C).

BECKWITH–WIEDEMANN SYNDROME

Owing to the association of MHL with Beckwith–Wiedemann syndrome,[3,4] germline DNA from both children was analyzed with the use of a methylation-specific multiplex ligation-dependent probe amplification mixture. Neither child had epigenetic abnormalities or copy-number alterations at chromosomal region 11p15.5. In Child 1, this finding was also supported by OncoScan results (Fig. S8 in the Supplementary Appendix). PCR amplification and Sanger sequencing of the three coding exons of *CDKN1C* in germline DNA from both children did not identify a pathogenic variant in either child (data not shown).

DISCUSSION

In this report, we describe a child with MHL that lacked tumor C19MC activation but instead harbored a germline truncating pathogenic vari-

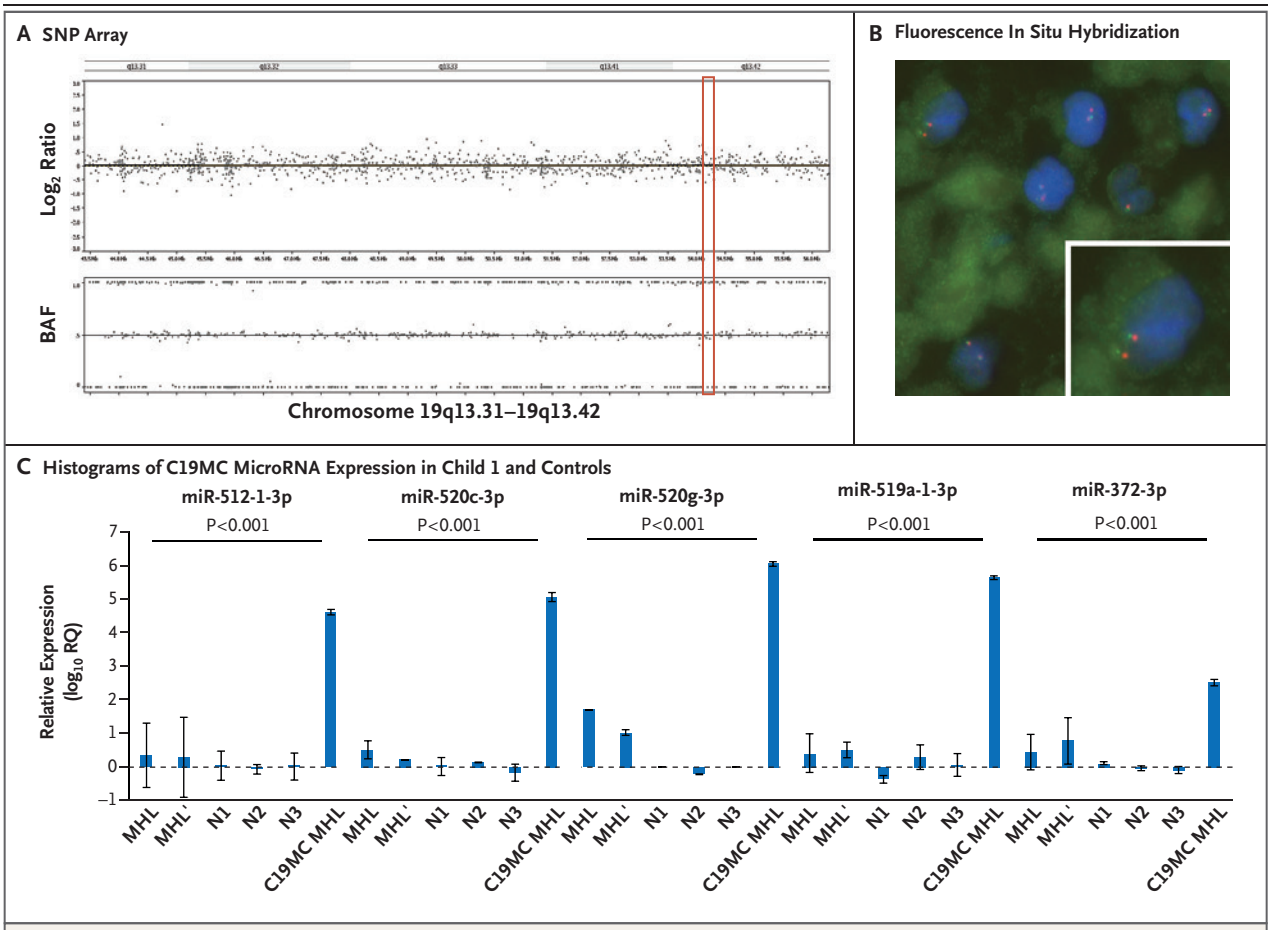

Figure 3. Chromosome 19q13 and C19MC MicroRNA Expression in Child 1's MHL.

Panel A shows the results of an OncoScan single-nucleotide polymorphism (SNP) array for chromosome 19q13 in a sample of MHL obtained during Child 1's first surgery, with the $\log_2$ ratio shown at the top and the B-allele frequency (BAF) shown at the bottom. On chromosome 19q13, neither copy-number alterations nor a copy-neutral loss of heterozygosity was detected. The C19MC region is marked with a red rectangle. Panel B shows representative interphase nuclei of Child 1's MHL from the first surgery that was hybridized with the 19q13 break-apart fluorescence in situ hybridization (FISH) probe. Interphase cells show two green–red fusion (yellow) signals, indicating no break in chromosomal region 19q13. The inset shows one interphase nuclei in detail. Owing to sectioning artifacts, some signals may be missing. The location of the microRNAs within C19MC and a nearby region are shown in Figure S9 in the Supplementary Appendix. Panel C shows histograms of the relative levels of C19MC microRNA expression measured by quantitative PCR assay in two MHL samples from Child 1 (MHL from the first surgery and MHL´ from the second surgery), normal liver samples (N1, N2, and N3) from three separate persons, and an MHL with C19MC activation (C19MC MHL). MHL samples from Child 1 had lower microRNA expression than the positive MHL. The standard deviations of the cycle thresholds are plotted as I bars. Bonferroni-corrected P values for the comparison between MHL samples (MHL and MHL´) and C19MC MHL are shown; all P values are provided in Table S1 in the Supplementary Appendix.

ant and a somatic hot-spot mutation in *DICER1*. We describe a second child with a liver lesion consistent with MHL, several phenotypes associated with DICER1 syndrome, and a pathogenic germline *DICER1* variant. We previously reported a four-amino-acid deletion resulting in a similar protein change (p.N1741_1744del) in a child with cystic nephroma, multinodular goiter, and a lung cyst,[16] all of which were present in Child 2. In Child 2 and the previously reported case,[16] the pathogenic germline variants affected highly conserved amino acids in the RNase IIIb domain[9] (Fig. S7 in the Supplementary Appendix) and appeared to similarly alter DICER1 function.

We and others have also shown that p.E1705Q is present in other DICER1 syndrome–related tumors.[12,17]

Before this study, the aberrant expression of C19MC microRNAs, due either to rearrangement of 19q13 or to androgenetic–biparental mosaicism, had been identified as the characteristic abnormality causing MHL.[5,6,8] Our data suggest that MHL can also be caused by *DICER1* mutations and is a phenotype of DICER1 syndrome. DICER1 is an RNase that is critical in the biogenesis of microRNAs.[9] Therefore, we hypothesize that mutations in *DICER1* dysregulate microRNA expression, promote hamartoma growth, and result in the formation of MHL. Deletion of *Dicer1* in mouse hepatocytes results in spontaneous development of hepatocellular carcinoma,[15] and several microRNAs have been shown to play a relevant role in liver development.[14,15,18]

In Child 1's MHL, from which we had sufficient tissue for analysis, we found neither chromosomal translocations nor androgenetic–biparental mosaicism and no activation of five C19MC microRNAs, findings that ruled out the recognized causes of MHL. We also observed that in Child 1's MHL the expression of certain liver-expressed microRNAs was altered, presumably because of the two *DICER1* mutations. Specifically, miR-122, a microRNA critically implicated in hepatocyte maturation and differentiation, was significantly down-regulated as compared with the normal liver tissues and with a non-*DICER1* MHL with C19MC expression. Down-regulation of miR-122 has been seen in hepatoblast-specific *DICER1* conditional knockout mice and in liver diseases.[15,18] Moreover, let-7, which is a regulator of cellular differentiation, was significantly down-regulated as compared with the non-*DICER1* control MHL. We also observed a significant up-regulation of miR-199b and miR-200a in MHL samples as compared with normal liver samples. Both microRNAs have been implicated in liver disease.[14] Although different microRNAs are involved in DICER1-driven MHL, the resulting microRNA perturbations could mimic the aberrant microRNA activation reported in C19MC-driven MHL. This notion of a common pathway to disease initiated by C19MC activation or *DICER1* mutations is supported by a recent study[19] showing pathogenic germline and somatic *DICER1* variants in two infantile brain tumors that resemble embryonal tumors with multilayered rosettes caused by C19MC overexpression.[20]

The relationship between MHL and its malignant counterpart, undifferentiated embryonal sarcoma,[4] resembles that seen between the subtypes of pleuropulmonary blastoma. Type I pleuropulmonary blastoma consists of primitive mesenchymal cells and cysts, and sarcomatous overgrowth of the cysts by the primitive cells leads to solid tumor formation (types II and III pleuropulmonary blastoma).[21] Before the entity of pleuropulmonary blastoma was established, some of these tumors were considered to be mesenchymal cystic hamartomas of the lung.[22] Another example of hamartoma characteristic of DICER1 syndrome is nasal chondromesenchymal hamartoma.[23] In addition, we found that Child 2's cystic hepatic mass regressed (Fig. S4 in the Supplementary Appendix), a finding that has been reported to occur in MHL.[4] Moreover, we found in Child 2 the regression of bilateral renal cysts, which has not been previously reported in DICER1 syndrome (Fig. S4 in the Supplementary Appendix); more longitudinal data are needed to help guide intervention decisions for such cysts.

In conclusion, MHL may be associated with both germline and somatic mutations in *DICER1* in the absence of chromosomal translocations involving 19q13.4 or aberrant activation of C19MC microRNAs.

Supported by a grant from the Canadian Institutes of Health Research (FDN-148390, to Dr. Foulkes), a grant from the C[17] Research Network/Childhood Cancer Canada Foundation (to Dr. Foulkes), a Garber Family Post Doctorate Fellowship in Hereditary Cancer (to Dr. Apellaniz-Ruiz), and grant support for infrastructure by KinderKrebsInitiative Buchholz/Holm-Seppensen (to Dr. Siebert). Dr. Kettwig was supported at the Göttinger College for Translational Medicine by the Lower Saxony Ministry of Science and Culture.

Disclosure forms provided by the authors are available with the full text of this article at NEJM.org.

We thank the patients and their families for their participation in this study; Peter Metrakos, M.D., and Anthoula Lazaris, Ph.D. (Research Institute of the McGill University Health Centre Liver Disease Biobank), for their help in obtaining the control liver samples used in this study; Nada Jabado, M.D., Ph.D., for sharing tissue from the MHL expressing C19MC; Barbara Rivera, Ph.D., and Leanne de Kock, Ph.D., for scientific input; and Celia M.T. Greenwood, Ph.D., and Amadou Diogo Barry, Ph.D., for statistical advice.

REFERENCES

1. Rosado E, Cabral P, Campo M, Tavares A. Mesenchymal hamartoma of the liver — a case report and literature review. J Radiol Case Rep 2013;7:35-43.
2. Ferrell LD, Kakar S, Terracciano LM, Wee A. Tumours and tumour-like lesions of the liver. In: Burt AD, Ferrell LD, Hübscher SG, eds. MacSween's pathology of the liver. 7th ed. Philadelphia: Elsevier, 2018:843-4.
3. García-de-la-Torre JP, Sotelo-Rodríguez MT, Santos-Briz A, Rodríguez-Peralto JL, De-Castro J. Mesenchymal hamartoma of the liver in Beckwith-Wiedemann syndrome: the first reported case. Pediatr Pathol Mol Med 2000;19:455-60.
4. Stringer MD, Alizai NK. Mesenchymal hamartoma of the liver: a systematic review. J Pediatr Surg 2005;40:1681-90.
5. Kapur RP, Berry JE, Tsuchiya KD, Opheim KE. Activation of the chromosome 19q microRNA cluster in sporadic and androgenetic-biparental mosaicism-associated hepatic mesenchymal hamartoma. Pediatr Dev Pathol 2014;17:75-84.
6. Keller RB, Demellawy DE, Quaglia A, Finegold M, Kapur RP. Methylation status of the chromosome arm 19q MicroRNA cluster in sporadic and androgenetic-biparental mosaicism-associated hepatic mesenchymal hamartoma. Pediatr Dev Pathol 2015;18:218-27.
7. Noguer-Dance M, Abu-Amero S, Al-Khtib M, et al. The primate-specific microRNA gene cluster (C19MC) is imprinted in the placenta. Hum Mol Genet 2010;19:3566-82.
8. Mathews J, Duncavage EJ, Pfeifer JD. Characterization of translocations in mesenchymal hamartoma and undifferentiated embryonal sarcoma of the liver. Exp Mol Pathol 2013;95:319-24.
9. Foulkes WD, Priest JR, Duchaine TF. DICER1: mutations, microRNAs and mechanisms. Nat Rev Cancer 2014;14:662-72.
10. Khan NE, Bauer AJ, Schultz KAP, et al. Quantification of thyroid cancer and multinodular goiter risk in the DICER1 syndrome: a family-based cohort study. J Clin Endocrinol Metab 2017;102:1614-22.
11. Wu MK, de Kock L, Conwell LS, et al. Functional characterization of multiple DICER1 mutations in an adolescent. Endocr Relat Cancer 2016;23(2):L1-L5.
12. Apellaniz-Ruiz M, de Kock L, Sabbaghian N, et al. Familial multinodular goiter and Sertoli-Leydig cell tumors associated with a large intragenic in-frame *DICER1* deletion. Eur J Endocrinol 2018;178(2):K11-K19.
13. de Kock L, Bah I, Revil T, et al. Deep sequencing reveals spatially distributed distinct hot spot mutations in DICER1-related multinodular goiter. J Clin Endocrinol Metab 2016;101:3637-45.
14. Hayes CN, Chayama K. MicroRNAs as biomarkers for liver disease and hepatocellular carcinoma. Int J Mol Sci 2016;17:280.
15. Chen Y, Verfaillie CM. MicroRNAs: the fine modulators of liver development and function. Liver Int 2014;34:976-90.
16. Rath SR, Bartley A, Charles A, et al. Multinodular goiter in children: an important pointer to a germline DICER1 mutation. J Clin Endocrinol Metab 2014;99:1947-8.
17. Yoo SK, Lee S, Kim SJ, et al. Comprehensive analysis of the transcriptional and mutational landscape of follicular and papillary thyroid cancers. PLoS Genet 2016;12(8):e1006239.
18. Filipowicz W, Grosshans H. The liver-specific microRNA miR-122: biology and therapeutic potential. Prog Drug Res 2011;67:221-38.
19. Uro-Coste E, Masliah-Planchon J, Siegfried A, et al. ETMR-like infantile cerebellar embryonal tumors in the extended morphologic spectrum of DICER1-related tumors. Acta Neuropathol 2019;137:175-7.
20. Kleinman CL, Gerges N, Papillon-Cavanagh S, et al. Fusion of TTYH1 with the C19MC microRNA cluster drives expression of a brain-specific DNMT3B isoform in the embryonal brain tumor ETMR. Nat Genet 2014;46:39-44.
21. Dehner LP, Messinger YH, Schultz KA, Williams GM, Wikenheiser-Brokamp K, Hill DA. Pleuropulmonary blastoma: evolution of an entity as an entry into a familial tumor predisposition syndrome. Pediatr Dev Pathol 2015;18:504-11.
22. Mark EJ. Mesenchymal cystic hamartoma of the lung. N Engl J Med 1986;315:1255-9.
23. Stewart DR, Messinger Y, Williams GM, et al. Nasal chondromesenchymal hamartomas arise secondary to germline and somatic mutations of DICER1 in the pleuropulmonary blastoma tumor predisposition disorder. Hum Genet 2014;133:1443-50.